Journal of Manufacturing Processes 74 (2022) 28–39

Contents lists available at ScienceDirect

Journal of Manufacturing Processes

journal homepage: www.elsevier.com/locate/manpro

The influence of the backing plate materials on microstructure and mechanical properties of friction spot extrusion brazing of AA2024-T3 aluminum alloy and Brass sheets

Moslem Paidar [a,*], Dmitry Bokov [b], Sadok Mehrez [c,d], Mahyuddin K.M. Nasution [e,*], Olatunji Oladimeji Ojo [f], Azlan Mohd Zain [g]

[a] Department of Materials Engineering, South Tehran Branch, Islamic Azad University, Tehran 1459853849, Iran
[b] Institute of Pharmacy, Sechenov First Moscow State Medical University, 8 Trubetskaya St., bldg. 2, Moscow 119991, Russian Federation
[c] Department of Mechanical Engineering, College of Engineering at Al Kharj, Prince Sattam bin Abdulaziz University, 16273, Saudi Arabia
[d] Department of Mechanical Engineering, University of Tunis El Manar, ENIT, BP 37, Le Belvédère, 1002 Tunis, Tunisia
[e] Data Science & Computational Intelligence Research Group, Universitas Sumatera Utara, Medan 20155, Indonesia
[f] Department of Industrial and Production Engineering, Federal University of Technology Akure, Akure, Nigeria
[g] UTM Big Data Centre, School of Computing, Universiti Teknologi Malaysia, 81310 Skudai Johor, Malaysia

ARTICLE INFO

Keywords:
Friction spot extrusion brazing
AA2024-T3 aluminum alloy
Brass
Backing plate
Fracture load

ABSTRACT

In this study, the impact of the backing plate materials on microstructural and mechanical features during friction spot extrusion brazing of AA2024-T3 aluminum alloy and brass sheets by inserting Zn as an interlayer was investigated. Results indicated that the change of the backing plate material influentially affected the microstructure of the reaction layers at the interface of the AA2024/Zn/brass joint. Besides, it was found that the Zn interlayer could restrict the creation of deleterious intermetallic compounds at the interface. Moreover, the attained data revealed that the weld produced by the steel backing plate raised the fracture load of the joint in comparison to the other weld obtained by the copper backing plate by 35% even though the peak temperature was enhanced with a change in the backing plate material from copper to steel. The improvement in the tensile result of the steel backing plate-produced joint is owing to the good metallurgical bonding (complete filling of the pre-threaded hole) and presence of a larger amount of Al-Zn eutectic phase at the brazed zone.

1. Introduction

The dissimilar joining of alloys like Aluminum (Al) to Brass or Copper is extensively used in many industries such as electronic and automotive industries owing to their excellent properties and economic advantages with the aim of heat conductivity enhancement and increasing the mechanical properties of the welds. However, joining of these alloys with the use of traditional welding processes is inordinately challenging owing to the generation of brittle intermetallic compound (IMCs) [1], porosity, or cracking that are disastrous on the Al-Brass interface [2]. These problems could be solved via alternative welding processes for welding of aluminum to brass such as ultrasonic spot welding (USW), Friction Stir Welding (FSW), Friction Stir Spot Welding (FSSW), Modified Friction Stir clinching (MFSC), Dieless Friction Stir Extrusion (DFSE) are the most common solid-state joining techniques [3]. However, the use of interlayer can act as a barrier and restrict the formation of deleterious IMCs phase at the interface. Abdollahzadeh et al. [2] reported that the addition of the interlayer during FSW can form a large solid solubility between aluminum and Zinc and in fact, prevent the further reaction between base alloys. Recently, Paidar et al. [4,5] studied the feasibly of Dieless Friction Stir Extrusion-Brazing (DFSE-B) and Friction spot extrusion welding-brazing for joining of pure copper to aluminum alloy with the aid of Zn as an interlayer. It was found that using zinc during the process resulted in the suppression of the flow-induced flaws and improved load-bearing performance of the dissimilar AA2024-T3/copper joints in comparison to the conventional FSSW. In addition to this, Kar et al. [6] studied the impact of the Nb as an interlayer during welding of Al to Ti through the FSW process. It was concluded that the existence of the Nb as an interlayer during welding influenced the microstructural changes and restrained the formation of

* Corresponding authors.
E-mail addresses: m.paidar@srbiau.ac.ir (M. Paidar), mahyuddin@usu.ac.id (M.K.M. Nasution).

https://doi.org/10.1016/j.jmapro.2021.12.002
Received 22 August 2021; Received in revised form 2 December 2021; Accepted 3 December 2021
Available online 9 December 2021
1526-6125/© 2021 The Society of Manufacturing Engineers. Published by Elsevier Ltd. All rights reserved.

Table 1
Chemical composition of AA2024-T3 alloy (wt%).

Alloy	Cu	Si	Mg	Mn	Cr	Al
AA2024-T3	4.9	0.43	1.28	0.629	0.012	Bal.

Table 2
Chemical composition of Brass (wt%).

Alloy	Cu	Zn	Fe	Pb	P
Brass	Bal.	38.16	0.16	0.09	0.01

detrimental IMCs in the weld zone.

In recent years, many researchers have investigated the impact of the various backing plate during FSW/FSSW/FSP, because the mechanical properties and microstructure of joints mainly depend on the thermal history during FSW [7]. Zhang et al. [7] investigated the effect of copper, steel, and granite backing plate materials during FSW of 2024-T3 aluminum alloy sheets on microstructure and properties of the welds. It was found that there was an inverse correlation between backplate diffusivity and heat input generation. The backing plate with low diffusivity efficaciously increased the heat input to the workpiece during the process and subsequently resulted in the enhancement of the sizes of equiaxed recrystallized grains in the weld zone. Raja et al. [8] studied the influence of the backing plate on tensile strength and microstructural changes during the FSW of the AA2014-T6 aluminum alloy. The authors deduced that the backing plate material was one of the most important parameters to control the quality of the welds. The Ti and Mild Steel (MS) backing plates were used in this investigation. It was discovered that the average grain size for the weld prepared by Ti and MS backing plate was 4.3 μm, while for the weld made by MS backing plate was 3.1 μm. Therefore, the joint prepared by MS indicated the highest tensile strength.

A Friction spot extrusion brazing process establishes mechanical interlocks between overlapped sheets (having an interlayer between them) by employing the downward plunging action of a rotating probeless tool to form an extrusion of the upper sheet into a prefabricated hole in the lower sheet. The interlayer decreases the reaction between the reactive base alloys and further creates a brazing area via a self-reacting mechanism to increase the joint's bonded width during the friction stir processing period. However, the application of this technique in joining aluminum and brass is yet to be thoroughly expounded in the literature. Thus, this paper focuses on the application of the Friction spot extrusion brazing process in joining AA2024-T3 and brass with a Zn foil as an interlayer medium to aid the brazing of the dissimilar metals. The influence of a change in the backing plate materials on the weld interface, bonding, and tensile-shear behaviors of the friction spot extrusion brazed AA2024/Zn/brass joint is investigated in this study.

2. Experimental setup

In this work, 1.5 thick Brass and 1.6 mm thick AA2024-T3 aluminum alloy were employed as lower and upper sheets respectively to generate FSEB joints by use of Zn (thickness of 50 μm) as interlayer. Tables 1 and 2 display the chemical composition of starting materials obtained via Quantometer Analysis. The principle of the FSEB process is demonstrated schematically in Fig. 1a and b. A pre-threaded hole with a 4 mm diameter is drilled in the lower sheet (Brass). A rotating prob-less tool leads to the generation of the frictional heat and subsequently forging (extruding) of the upper sheet (AA2024-T3) into the pre-fabricated hole. To diminish the impact of the deleterious IMCs at the Al/Brass joints and to avoid/limit ample reaction between base alloys, a Zn interlayer was applied in between Al and brass sheets.

Before the FSEB process, the faying surfaces of Al, Brass, and Zn interlayer were mechanically ground with the aid of 400 grid SiC emery papers and then cleaned with acetone. The FSEB was conducted with a milling machine (FP4MK) under constant welding parameters (tool rotational speed of 1000 rpm, shoulder plunge depth of 0.3 mm, dwell time of 10 s) on the backing plates of steel (Fe) and copper (Cu). It is worth mentioning that the tool is composed of H13 tool steel having 14 mm diameter was employed for the FSEB process (see Fig. 1c). To

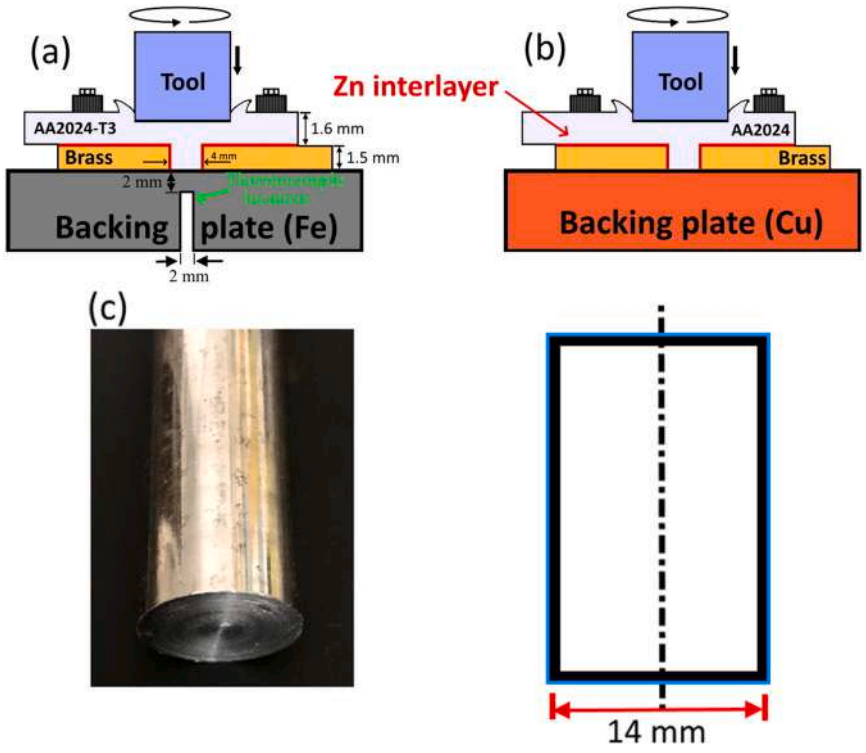

Fig. 1. Schematic of FSEB technique with (a) copper and (b) steel anvils, (c) tool used in this investigation.

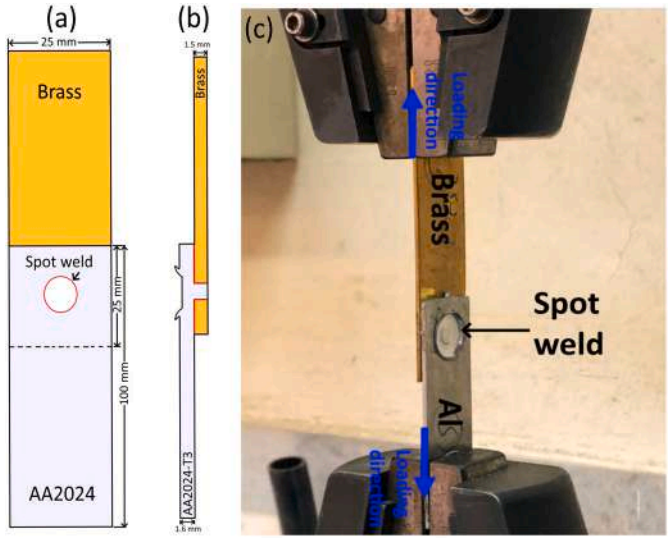

Fig. 2. Dimensions of the tensile-shear test (the arrows depict the loading direction), and (b) tensile test machine.

measure the temperature distribution of the welds made by the FSEB process, a K-type thermocouple was positioned in the backing plates. The exact location of the thermocouple during the process is indicated in Fig. 1a. To identify the microstructure and phase formed at the weld interface, the cross-section of the welds was ground, polished, and then electrically etched by Barker's reagent for 90 s at 20 V for Al alloy, whereas brass alloy was etched using a 50 HCl, 5 g $FeCl_3$ and 100 mm water, for 5 s at 10 V. The microstructure of the welds was explored by scanning electron microscope (SEM) equipped with an energy-dispersive spectrometer (EDS), optical microscopy (OM) and transmission electron microscope (TEM). The weld specimens for TEM were prepared via standard metallurgical preparation procedures followed by ion beam etching in a precision ion polishing system with liquid nitrogen.

The JEOL JEM 2100 TEM was employed to obtain the BF (bright field) images of the welds. To assess the role of the backing plate materials on fracture load of the joints, the tensile-shear test was performed with the use of a universal testing machine (INSTRON 5500R) at a strain velocity of 5 mm/min. The dimensions of the tensile-shear test samples based on AWS C1.1 standard are represented in Fig. 2a-c and d. To understand the influence of the backing plates material on the phases formed at the brass/AA2024 interface, X-ray diffraction (XRD) analysis was employed on the fracture surfaces of the failed samples. For the XRD test, Cu target was employed while the utilized voltage and current were 45 kV and 40 mA respectively.

3. Results and discussion

3.1. Surface appearance and macrostructure characteristics

The typical FESEM macrographs of the FSEBed Brass/Zn/Al joints using steel and copper backing plates along with surface appearance are revealed in Fig. 3. Backing plate materials is a pivotal factor that affects the macrostructure of the joints during the FSEB process. Worthy of note is that the presence of Zn interlayer during the process led to the formation of brazed zones at the edges of the joints (beneath the shoulder indentation) between aluminum and brass alloys, as highlighted by yellow rectangular boxes in Fig. 3a and b, regardless of the backing plate materials. This implies that the Zn interlayer has completely melted during the FSEB process of AA2024 to brass. Paidar et al. [4] reported that the induced brazing increased the stress-bearing area (brazed + stir regions) and this occurrence resulted in the improvement of the fracture

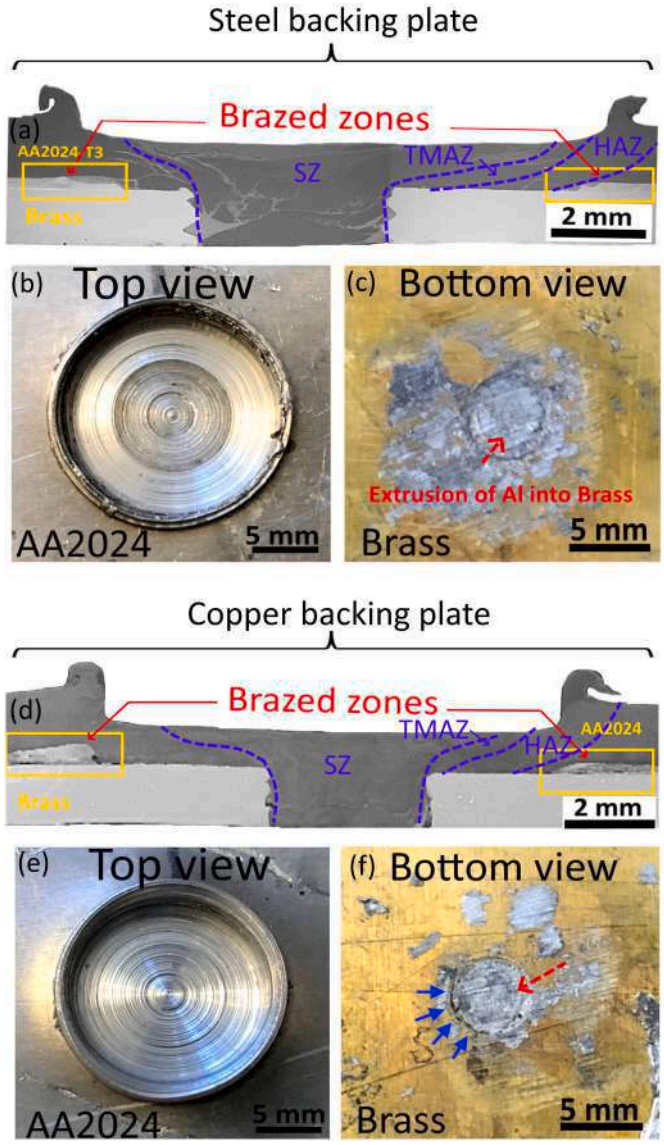

Fig. 3. FESEM cross-sectional images and surface appearance of the weld made by various backing plate materials, (a) cross-section, (b) top view, and (c) back view of weld with steel backing plate, while (d) cross-section, (e) top view, (f) back view of weld with copper backing plate. (For interpretation of the references to color in this figure, the reader is referred to the web version of this article.)

load of the dissimilar joints. The important point to note here is that defect-free weld was obtained for the joint made with steel backing plate, whereas for the weld made by copper backing plate some interfacial defects were formed at the brazed zones. The root cause for this occurrence can be attributed to the higher peak temperature in the weld made by the steel backing plate in comparison with the weld produced by copper backing. The temperature histories of the welds are provided in Fig. 4, with the peak temperatures of 448 and 354 °C in the joints fabricated with steel and Cu backing plates respectively. Owing to the lower thermal conductivity of steel (16 W/m·K) in comparison to the copper backing plate (410 W/m·K), less amount of heat (temperature) will be dissipated and a larger amount of heat will be retained in the weld fabricated with steel backing plate. As a result, the severity of the material's deformation, particularly AA2024, leads to the complete filling of the pre-threaded hole via downward movement (extrusion) of the AA2024-T3 towards the brass side [9]. This extrusion of AA2024-T3 into the brass thus creates the required mechanical interlocking

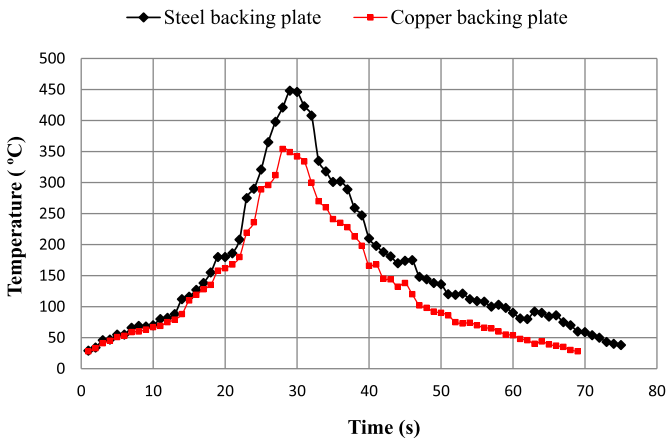

Fig. 4. Temperature histories of the welds.

characteristic in the AA2024/Zn/brass joints and thereby resulted in the complete filling of the pre-threaded hole (omission of the keyhole), which can be acutely worthy to improve the tensile/shear strength of the joints (see the red arrow in Fig. 3c). It is to be noted that a direct correlation exists between the peak temperature and the friction-induced heat input in FSSW/FSW joints. The higher peak temperature (heat input) in the weld made by the steel backing plate is considered to have aided a better material flow, and inevitably a better extrusion of the AA2024 alloy into the brass material is the outcome. On the contrary, with a copper backing, due to the higher thermal conductivity of copper, the amount of heat generated at the Al/Zn/brass joint would be different than that of weld produced by steel backing plate. Therefore, the small percentage of AA2024 can be extruded via downward movement of the probe-less shoulder and consequently resulted in the partial filling of the pre-threaded hole (see red arrow in Fig. 3f).

The surface appearances (top view and bottom view) of the joints produced by steel and copper backing plates are indicated in Fig. 3b, c, and e, f respectively. It can be seen from Fig. 3 that backing plate material did not considerably influence the top view (Al side) of the joints. However, the effect of the backing plate material on the bottom view of the joints confirmed the higher extruding (forging) of the AA2024-T3 towards brass.

By comparison with the copper backing, the steel backing had more influence on the frictional heat generated during the FSEB process, as obvious in Fig. 3c and f. The huge discrepancy in the thermal conductivities of copper and steel was the main reason for this occurrence. Indeed, owing to the higher thermal conductivity of copper, the FSEBed sample experienced a higher heat loss in comparison with that made by the steel backing plate. Park et al. [10] investigated the influence of backing plate in FSW of AA5082/AA5082 aluminum alloy. It was reported that there is a direct correlation between heat loss and the thermal conductivity of the backing plate material. These results indicated that appropriate deformation and stirring occurred in the joints using a steel (Fe) backing plate. This fact explains why the weld made by copper backing plate restrained the flowability of the materials (see blue arrows on Fig. 3f) and consequently resulted in a relatively weaker interfacial bonding and poor friction and plastic deformation-aided heat input during the FSEB process, between Al and Brass (see the green arrows on Fig. 3d). Such poor bonding at the brazed zone reduces the effective bonding width of the weld fabricated with the Cu backing plate. Thus, it can be concluded that the backing plate materials not only played a vital role in the brazing regions during the FSEB process but also resulted in the intense stirring action and subsequently controlled the extrusion of the upper sheet and could produce sound welds with the addition of a Zn interlayer.

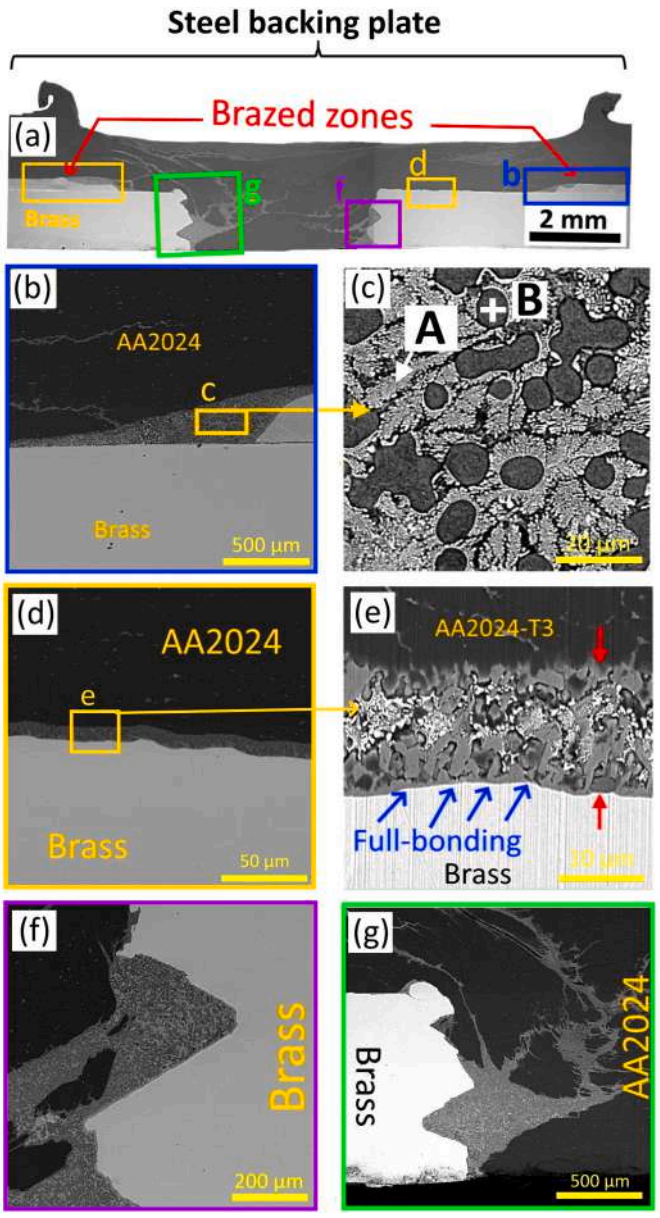

Fig. 5. FESEM micrographs of AA2024/Zn/brass joint produced by steel backing plate.

3.2. Microstructure features

Backing plate materials can be considered as one of the momentous factors to control the microstructure of the joints during the FSEB process. The microstructure of the weld produced by steel and copper backing plates is illustrated in Figs. 5 and 6 respectively. From Figs. 5b and 6b it is apparent that when the steel backing plate was used, a joint without any defect was generated at the brazed zones. It is well known that a steel backing plate displays a better joint than that of the weld made by a copper backing plate. The most likely reason for this interesting occurrence is largely owing to the disparity in the thermal conductivity of copper and steel metals. Since that the thermal conductivity of the steel is largely lower than that of the copper backing plate, thus a large amount of the heat would be retained at the AA2024/Zn/brass interface. In contrast, for the weld generated by the copper backing plate, a metallurgically unbonded area is formed at the brazed zones that can be ascribed to the upper sheet bulging-induced interfacial gap (see red circle in Fig. 6b). Saju et al. [11,12] reported that the upper sheet

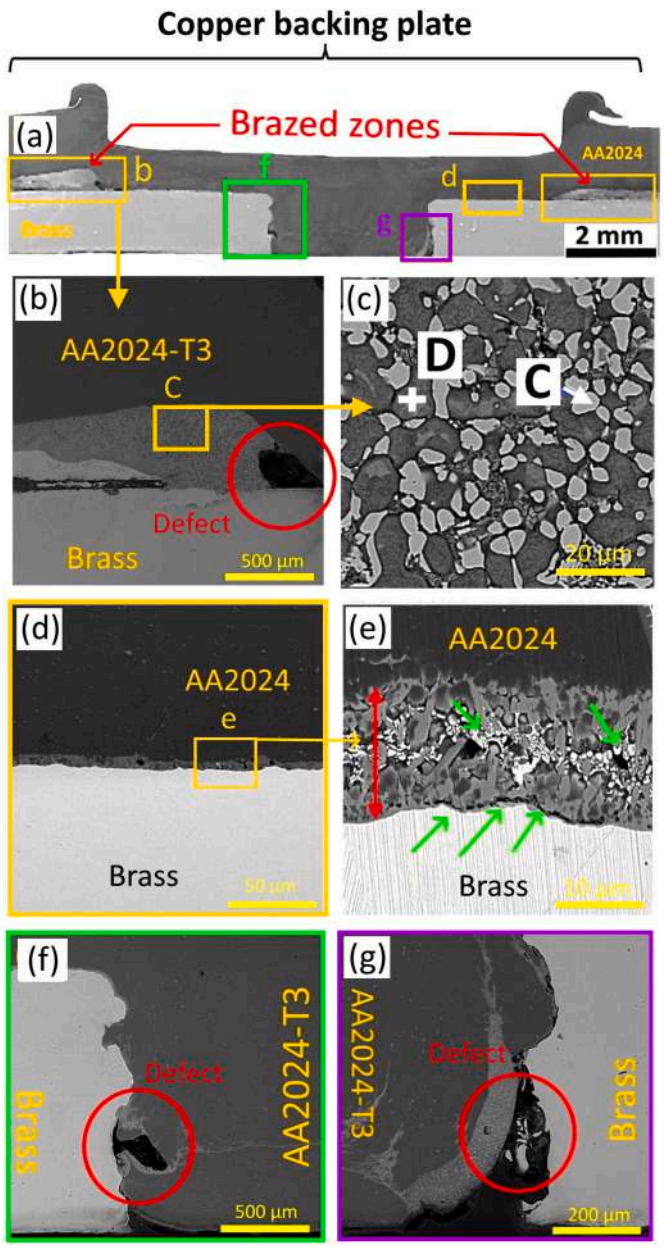

Fig. 6. FESEM micrographs of AA2024/Zn/brass joint produced by copper backing plate. (For interpretation of the references to color in this figure, the reader is referred to the web version of this article.)

bulging occurred as a result of the impact of fixture clamping on the upper sheet.

The high magnification views of the brazed zones are represented in Figs. 5c and 6c. It can be seen from Fig. 5c that Al-Zn eutectic structure was formed at the brazing zones. Paidar et al. [9] reported that owing to the more solubility of Al in Zn, the possible formation of the Al-Zn eutectic structure is more than that of the Cu-Zn eutectic at the interface. Among all elements, the solubility of Zn in Al has been acknowledged to be the largest (67 at.% at 654 K) [13]. According to Boucherit et al. [1,14], the higher equilibrium solubility of Al in Zn aids the formation of Al-Zn eutectic structure, than that of Cu in Zn. The average thicknesses of the brazed layers in the welds fabricated with steel and copper backing plates are 10.98 μm and 7.81 μm respectively. From Fig. 5c, it can also be observed that the brazed zone is composed of flower-like spirals (point A) and island-like structures (point B) with the use of a steel backing plate. Contrarily, for the weld generated using a copper backing plate no eutectic structure is created at the Al/brass interface. In other words, it can be said that the eutectic reaction of the molten Zn with Al and brass decreased as copper was used as a backing plate. As obvious in Fig. 6c, separated islands were formed at the brazed zone that is attributable to increased heat loss when a copper backing plate was used and led to the elimination of the eutectic structure of Al-Zn. The main cause for this phenomenon is unknown, but lower heat input when utilizing the copper backing plate can be the most likely reason for this interesting occurrence. However, it is worth noting that owing to the forging effect of the probe-less shoulder, the molten Zn interlayer pushed into the Al/brass interface. In fact, due to the presence of the molten Zn, the creation of deleterious IMCs like Al_4Cu_9 at the brazed zones is confined at the Al/brass interface.

To find out the chemical composition of the phase formed in the weld zone of both the steel and copper backing plates, the EDS analysis was carried out. The EDS results are provided in Fig. 7. The EDS results affirmed the presence of the lamellar Al-Zn eutectic structure during FSEB of AA2024 to brass. Results depicted that point A with a flower-like spirals structure (light grey phase in Fig. 5c) is composed of 29.92Al–2.34Cu–67.74 Zn (in at.%), whereas point B with an island-like structure is 12.61Al–4.81Cu–82.58 Zn (in at.%). Due to the high content of Al and Zn, points A and B belong to the Al-Zn solid phase [15]. Further, EDS analysis for the weld made via copper backing plate was conducted on the FSEBed Al-to-brass. Base on EDS results, it was found that point C with an island-like structure is 11.14Al–8.95Cu–79.91Zn (in at.%), like point B in Fig. 5c, while the point D is composed of 88.39Al–2.08Cu–9.53Zn (in at.%). According to these results, it can be concluded that Zn as an interlayer can limit the solid solubility of Cu in Al and indeed can restrict the detrimental impact of the IMCs at the AA2024/Zn/brass interface [16]. The presence of Zn inhibits the direct contact and reaction between Al and Cu elements to some extent while the high solubility of Al in Zn aids the formation Al-Zn phase instead of the deleterious IMCs.

Another striking feature observed in this investigation was the formation of the Al_2Cu phase between Al and brass adjacent prefabricated hole (see Figs. 5e and 6e). As mentioned earlier, owing to the presence of the Zn interlayer, the formation of brittle IMCs at the brazed zone was negligible. Although the vast majority of the molten Zn interlayer can be pushed into the prefabricated hole and even can remove from the edges of the joints, regardless of the backing plate materials. This was mainly associated with the extrusion force of the probe-less shoulder during the FSEB process. Thus, it can be asserted that the Zn interlayer had a negligible effect in the middle of the interface (see point d on Fig. 5a) and led to the formation of a small amount of $CuAl_2$ phase. Although Al-Zn eutectic and Cu-Zn phases are the possible composition of point C in Fig. 5e, the EDS analysis of point C also shows the presence of $CuAl_2$ IMCs (at.% 66.18Al–18.89Cu–14.93Zn) due to the high Al and Cu contents. The 14.93 at.% Zn is expected to form a eutectic structure with Al because Zn and Al do not form intermetallic phases [13].

Fig. 5f, g depict the complete formation of the prefabricated hole by upper sheet alloy (AA2024), whereas, for the weld made with the use of the copper backing plate, due to higher heat loss during the FSEB process, the joint will be subjected to lower plastic deformation (see Fig. 6f, g). Indeed, it can be reasoned that the use of the copper backing plate resulted in a large amount of heat dissipation (or temperature loss) away from the stir region. It can be seen in Fig. 5f and g that the high amount of the molten Zn is pushed into the prefabricated hole by the tool. Some of the molten Zn has been squeezed outward into the AA2024 aluminum alloy. Such a squeeze out of molten Zn (from the weld line) into the intergranular cracks was reported to have caused the liquid metal embrittlement [15].

Balasundaram et al. [15] have reported that liquid metal embrittlement can take place when ductile metals like Al or Cu are stressed while in contact with liquid metals (molten Zn). For clarity, the Al-Zn eutectic structure at the brazed zone of the AA2024/Zn/brass joint, the EDS map analysis of the weld was conducted (see Fig. 8). As was expected, due to

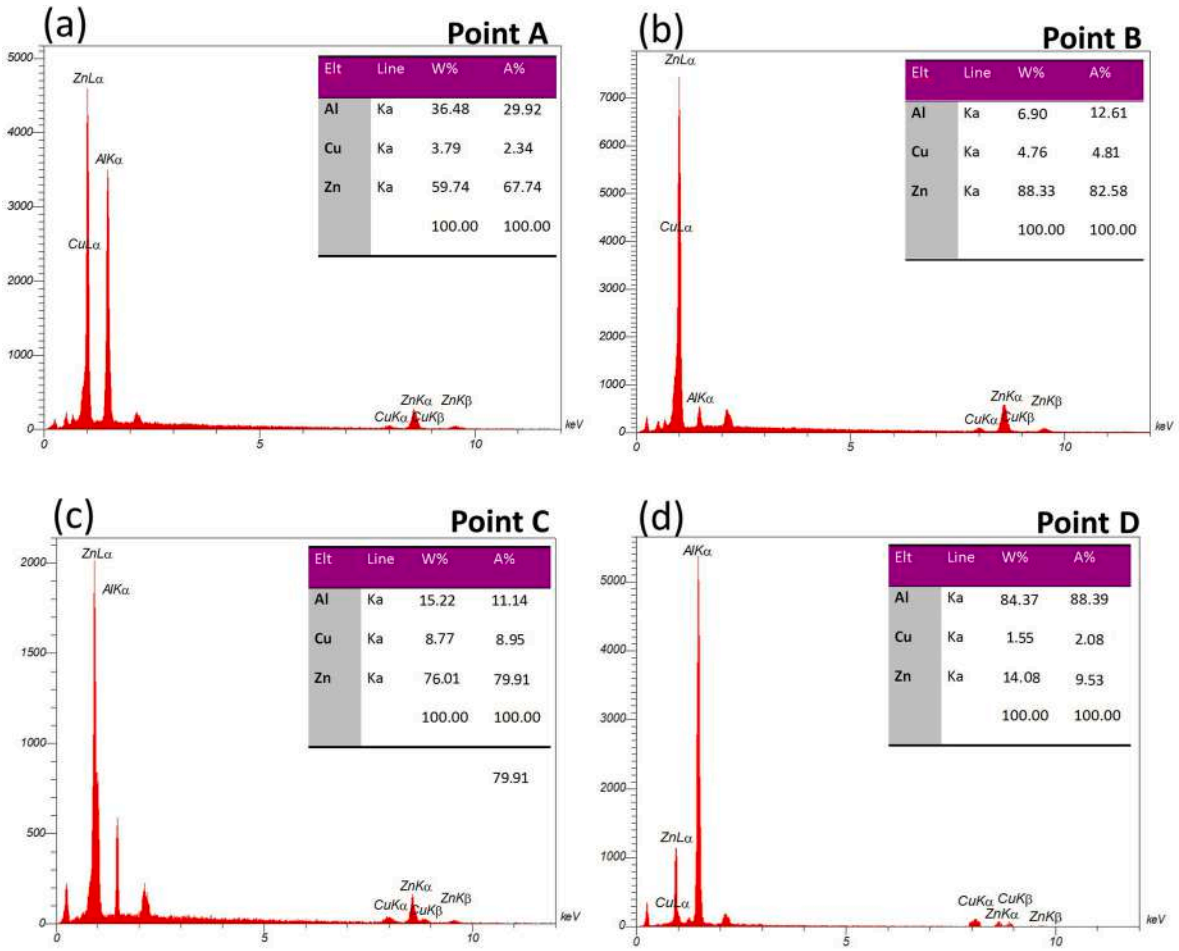

Fig. 7. EDS analyses of marked points of the AA2024/Zn/Brass joint with, (a), (b) steel, (c), (d) copper backing plate.

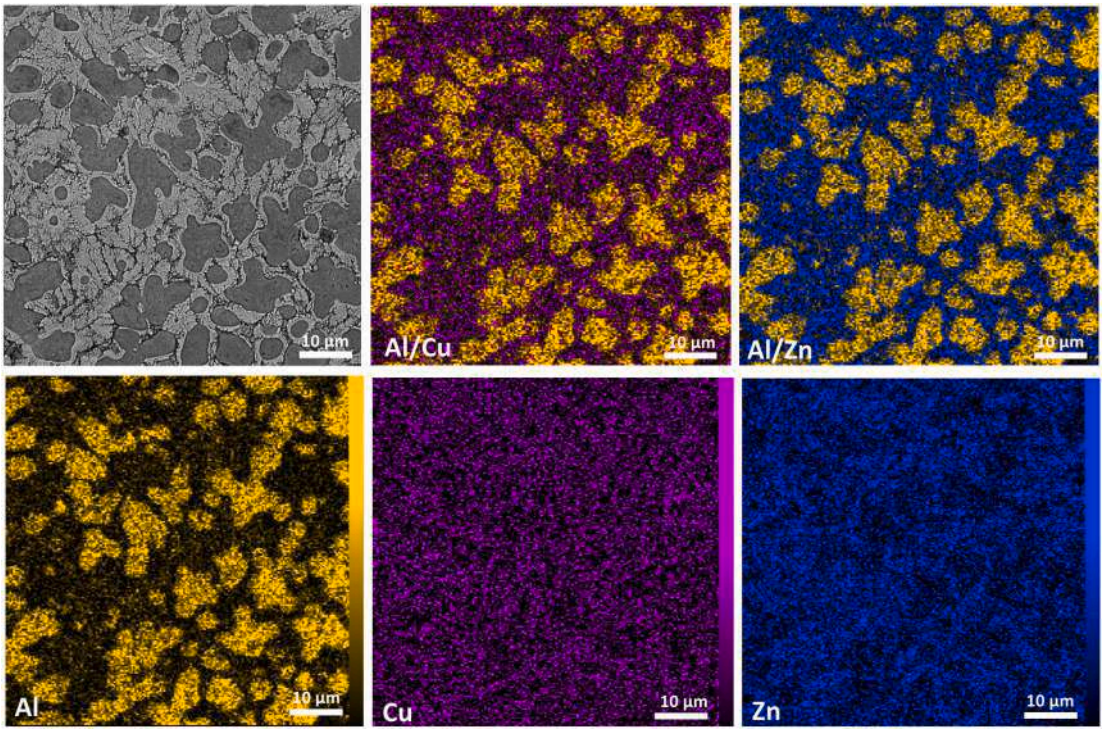

Fig. 8. EDS map of AA2024/Zn/brass weld prepared by steel backing plate.

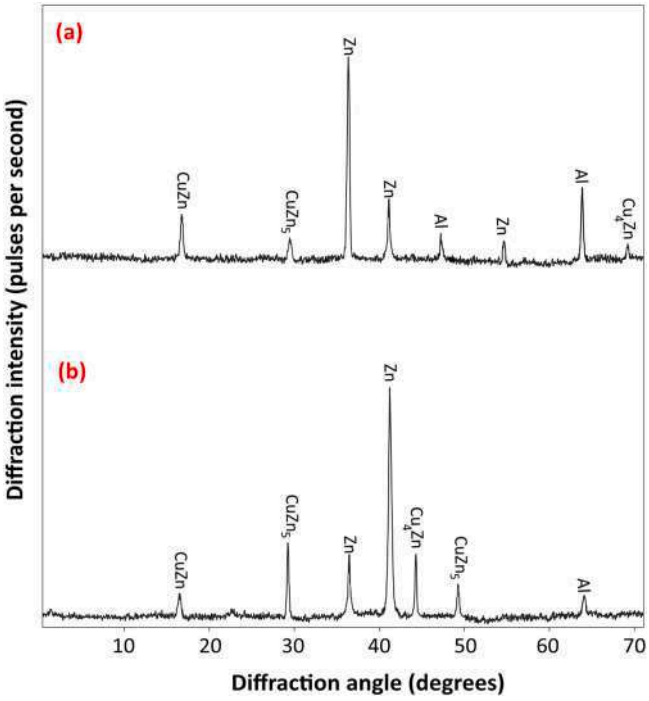

Fig. 9. XRD results of welds produced with (a) steel backing plate, (b) copper backing plate.

the high solubility of Al in Zn, the possibility of Al-Zn eutectic structure formation is more than that of the Cu-Zn eutectic at the interface. The XRD results provided in Fig. 9 have confirmed the formation of Cu-Zn phases (CuZn, $CuZn_5$, and Cu_4Zn) in the welds.

The optical microstructure of the various zones during the FSEB process for both steel and copper backing plates is represented in Fig. 10. The microstructure can be classified into three zones ranging from stir zone (SZ), thermomechanically affected zone (TMAZ) as well as heat-affected zone (HAZ). It is worth mentioning that the great disparity of these regions was in terms of the thermal history/cycle, plastic deformation, and subsequently grain size. It can be seen from this figure that the impact of the steel backing plate on the grain growth and plastic deformation was relatively more than that of the copper backing plate. The fine and equiaxed grains caused by the dynamic recrystallization [17–19] is the main feature of the SZ microstructure, while the TMAZ mainly consisted of elongated and severely deformed grains that can be stemmed from the tool-induced material flow [20] and severe plastic deformation [4], irrespective of the backing plate materials (see Fig. 10b). It is essential to note that owing to the higher thermal conductivity and in fact due to the production of inadequate heat input (heat loss) with the copper backing plate compared with steel, the joints are exposed to the lower temperature gradient and consequently, the grain growth was hampered. It can be reasoned that as the heat input decreases, grain growth decreases as a result of the faster cooling rate in the weld made by the copper backing plate. Liu et al. [21] have discovered that when the other welding parameters are the same, the thermal conductibility of the base alloy and backing plate materials can influence the heat input by changing the cooling rate as well as plastic deformation. It can be observed from Fig. 10b and c that using steel backing plate not only affected the microstructure of the SZ but also the grain size of TMAZ and HAZ were slightly larger in comparison to the joint produced via copper backing plate.

The grain size-frequency distribution of the FSEBed samples as a function of backing plate materials is displayed in Fig. 11. It was observed that the grain size of the joint made using a steel backing plate in the SZ was slightly coarser than that of the copper backing plate. This is an indication of higher heat input was obtained in the weld region with the use of steel backing plate and thereby resulted in lower heat loss during the FSEB process, which consequently increased the average grain size from 4.38 μm for the weld generated with the copper backing plate to 7.08 μm.

Forasmuch as the microstructure is one of the key factors that affect the mechanical behavior of the joints, thus the precipitate and dislocation characteristics of the SZ were revealed by FESEM and TEM. The influence of the backing plate materials on the precipitate sizes of the SZ was explored. Fig. 12a and b demonstrate the distribution of the precipitate in the SZ during the FSEB process. It is found that the size and distribution of the precipitates were mainly affected by backing plate materials. It can be seen from Fig. 12a and b that the number of precipitates for weld generated by steel backing plate was lesser than that of the copper backing plate. Using copper as the backing plate led to the

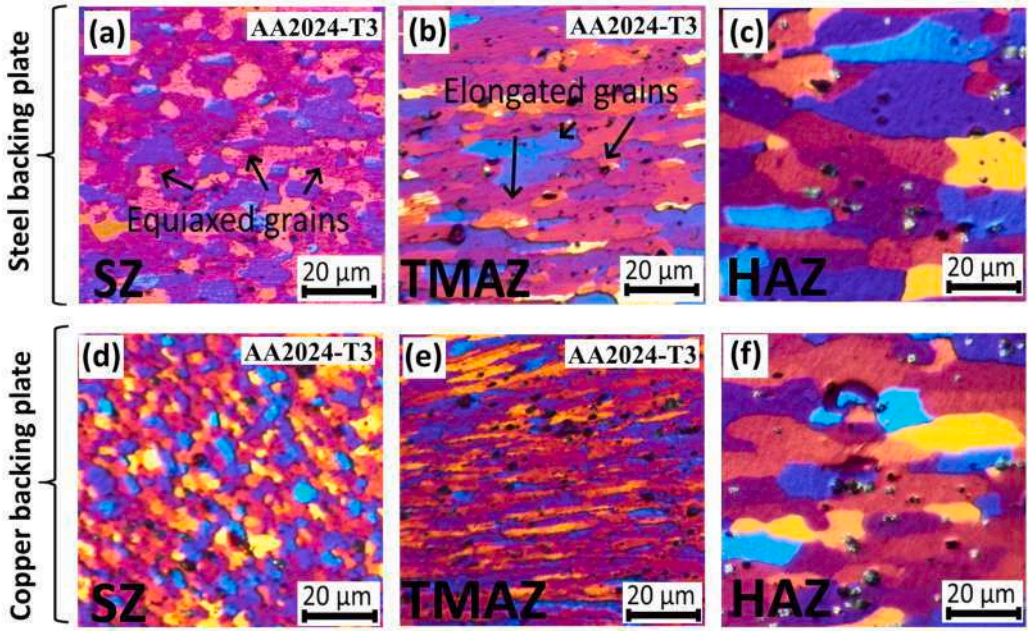

Fig. 10. Microstructure of various zones prepared at the AA2024 aluminum alloy side using different backing plates, (a–c) steel and (d–f) copper.

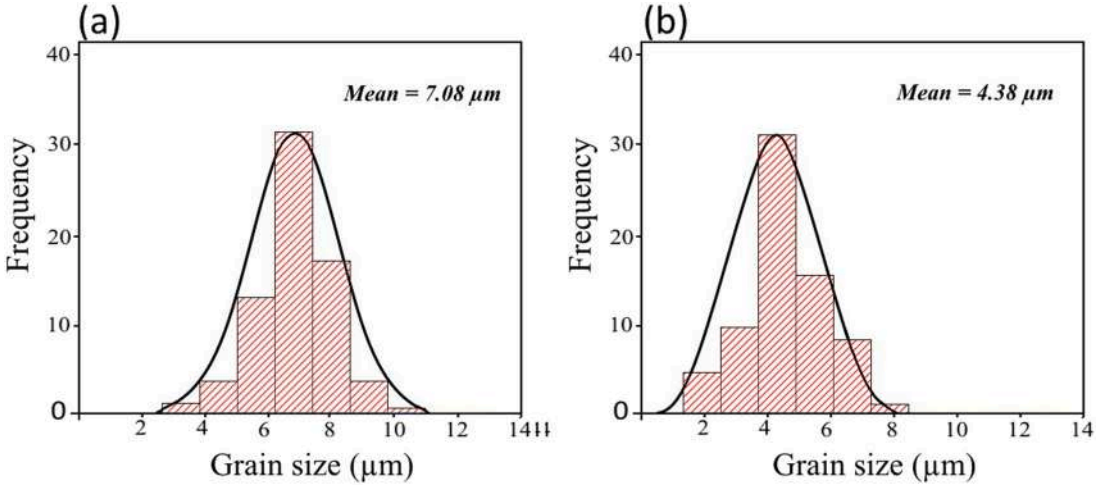

Fig. 11. Frequency distribution of the grain size in the stir zone with, (a) steel and (b) copper backing plates.

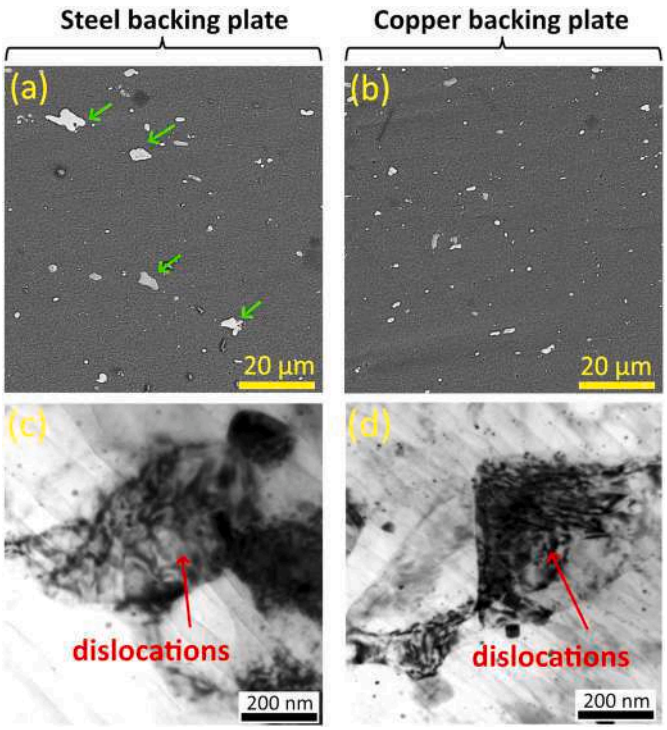

Fig. 12. FESEM and HRTEM images of the joints prepared by various backing plates, (a, c) steel and (b, d) copper backing plate. (For interpretation of the references to color in this figure, the reader is referred to the web version of this article.)

lower precipitate coarsening or reduced sizes of precipitate at the weld zone. On the contrary, large precipitates were observed for the weld produced using steel (see green arrows in Fig. 12a).

Additionally, as seen in Fig. 12b, the dispersion and size of the precipitates appeared much more uniform with the use of the copper plate as compared to that of the FSEBed joint using a steel backing plate that can be correlated to the proficiency of the copper plate in removing heat during the process. It reveals that the peak temperature of the Al/brass joint with copper backing plate was lower than that of the steel backing plate. The maximum temperature of the joints based on the grain size in the SZ can be calculated by the following equations [22]:

$$\mathrm{Ln}\,(D_{\text{stir zone}}) = 9.0\text{–}0.27\,\mathrm{Ln}\,(Z) \quad (1)$$

$$Z = \dot{\varepsilon}\exp\exp\left(\frac{Q}{RT}\right) \quad (2)$$

where D_{SZ} is the grain size of SZ, Q is the hot deformation activation energy, Z is the Zener-Hollomon parameter, $\dot{\varepsilon}$ is the strain rate, R is the gas constant and T is the SZ peak temperature. It is known that there is an inverse correlation between temperature SZ grain size (D) and Zener-Hollomon parameter (Z). Therefore, it can be concluded that the finer grain size will be formed with a high thermal conductivity material (copper) because the heat input produced in the joint using a steel backing plate was substantially larger than that of the copper plate.

The impact of the backing plate materials on the dislocations is indicated in Fig. 12c and d. It can be seen from TEM images that with a copper backing plate a large enhancement in the amount of the density of dislocations was observed inside the grains, which is obviously due to the higher heat loss during the FSEB process. Based on the results above, it can be said that the type of backing plate material was a contributing factor that affect the macro and microstructure of welds during FSEB. Steel backing plate aids thermal retention (or lesser thermal dissipation) in the weld and this occurrence aids grain growth and the formation of coarsened precipitates.

3.3. Microhardness and tensile/shear strength

Fig. 13 provides the hardness distribution across the welds fabricated with copper and steel backing plates. The average hardness values of the as-received brass and AA2024-T3 alloys are 89 and 108 HV respectively. Although the stirring/dynamic recrystallization effect of the FSEB process improved the microhardness at the weld center, the use of copper and steel as backing plates has a somewhat close impact on the microhardness distribution of the FSEB AA2024-T3/Zn/Brass joint. A slightly higher hardness value of 141 HV is obtained at the weld center of the joint fabricated with the copper backing plate as compared to the other weld (130 HV). This outcome can be related to the disparity in the average grain sizes of welds obtained with the steel and copper backing plates (see Fig. 11). However, the significant increase in the microhardness values at the weld center of joints, irrespective of the nature of the backing plate, is owing to grain refinement (Hall Petch relation) and the friction-assisted precipitation hardening at the stirred and extruded part (AA2024-T3) of the joint. Among the phases (θ-$CuAl_2$, S-Al_2CuMg, and α-Al) of the AA2024-T3 alloy, the S-Al_2CuMg phase is the strengthening phase [23,24] that is considered to have improved the hardness at the stirred and extruded root of the plasticized AA2024-T3 alloy.

The tensile/shear strength of welds produced with copper and steel

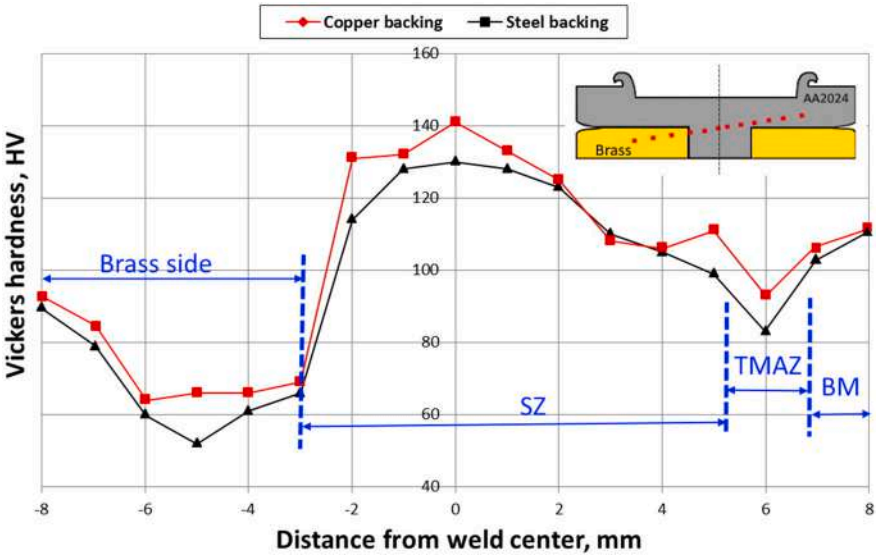

Fig. 13. Microhardness distribution across the welds as a function of backing plates.

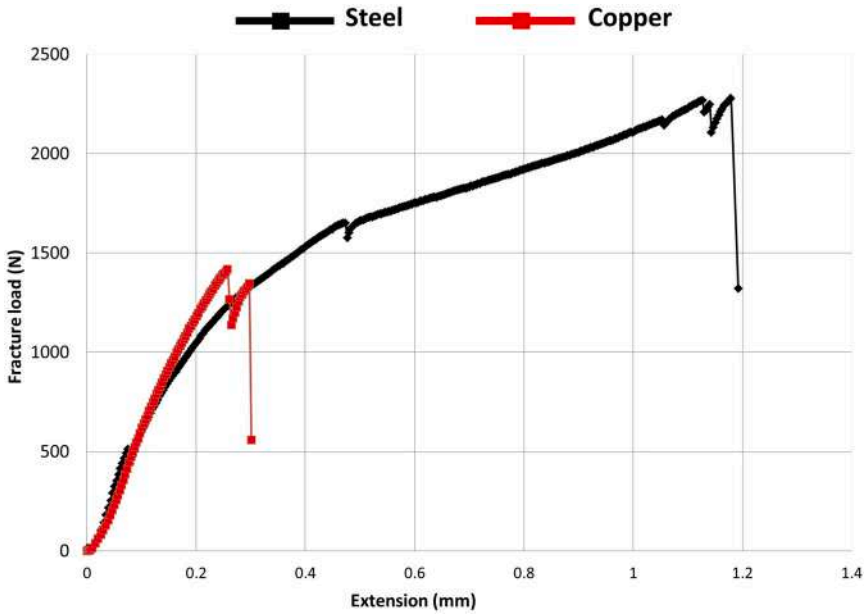

Fig. 14. Variations of fracture load versus extension with different backing plates.

backing plates is demonstrated in Fig. 14. It can be seen from Fig. 14 that backing plate materials had a crucial role in the fracture load and elongation of the joints obtained under copper and steel metals during FSEB of Al to brass with Zn as an intermediate material. It is found that with the use of the steel backing plate higher fracture load was obtained in comparison to the other weld gained by the copper backing plate. As can be seen, the fracture load of the dissimilar welding of brass to Al prepared with the utilization of steel backing plate was 2209 N, while the fracture load of 1437 N was gained when copper was used as backing. The variation of the fracture load with the backing plate can be attributed to the difference in the heat input as well as the complete filling of the pre-threaded hole via the downward movement (extrusion) of the upper sheet towards the lower sheet. As explained earlier, owing to the thermal conductivity of the Cu backing plate, the FSEBed sample experienced a higher heat loss and subsequently resulted in the deletion of Al-Zn eutectic structure in the brazed zone and also some defects at the brazed zone in comparison with that made by steel backing plate. The higher heat input and temperature gradient owing to the lower heat removal from the joint made by steel, lead to higher deformation/material flow and this consequently results in the complete filling-in and a flow-induced metallurgical bonding of Al to brass during the FSEB process. Using copper backing plate paltry affects the material flow and produced a small metallurgically unbonded region with a palpable flow-induced discontinuity at Al/Zn/brass interface. The weaker interfacial bonding (at the brazed zone) of the weld produced with the Cu backing plate could be said to have reduced the effective loadbearing region of the weld as compared to the other weld counterpart. This has contributed to the reduced weld strength of the joint produced with the Cu backing plate as against the weld fabricated with the steel backing plate. A large weld faying interface in the studies of Lei et al. [25] improved the tensile strength and ductility of the spot-welded AA6061-T6 joint. It can be concluded that a good interfacial bonding at the brazed zone of the weld (produced with the steel backing plate) is a salient factor responsible for a better failure load in the weld.

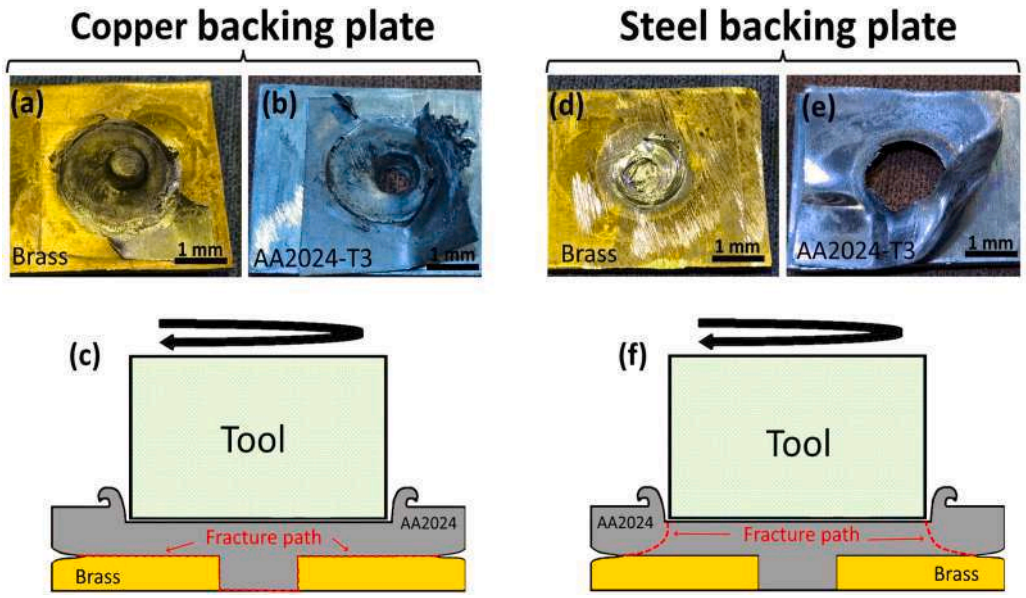

Fig. 15. Fracture surface and fracture path of FSEBed specimen with (a–c) copper and (d–f) steel backing plates. (For interpretation of the references to color in this figure, the reader is referred to the web version of this article.)

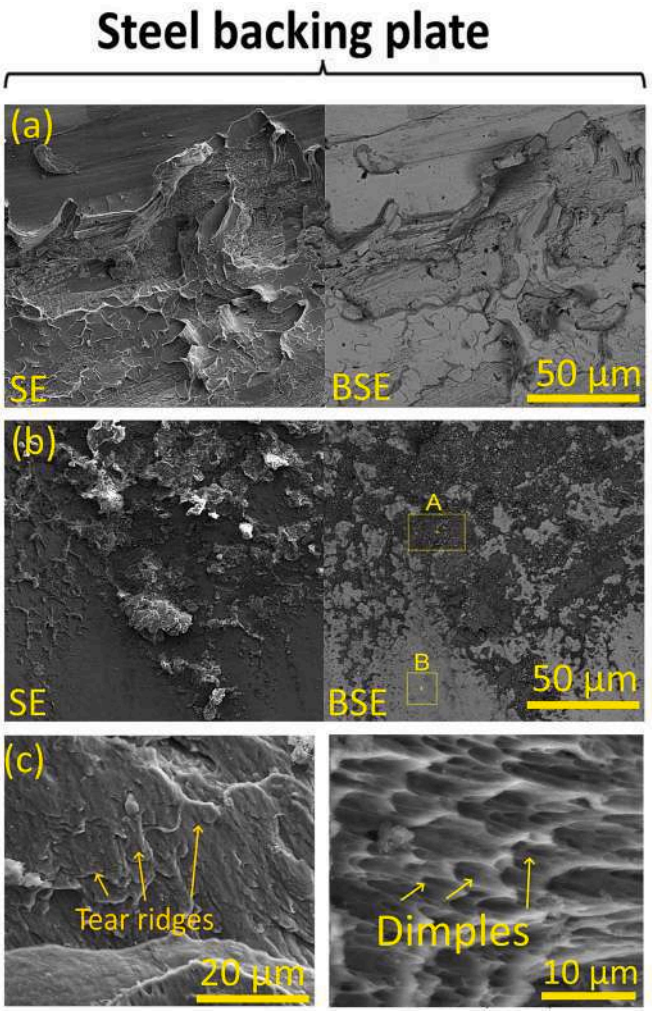

Fig. 16. FESEM fracture morphology of AA2024/Zn/brass joint prepared by steel backing plate.

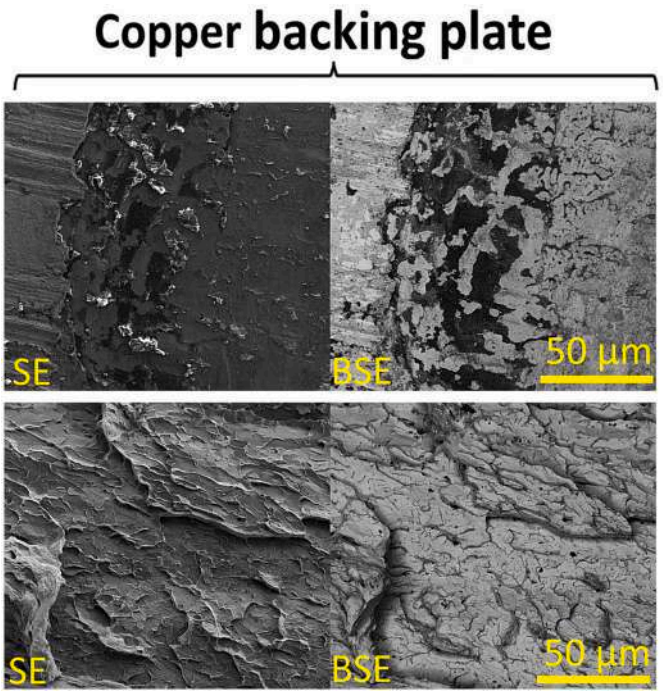

Fig. 17. FESEM fracture morphology of AA2024/Zn/brass joint prepared by the copper backing plate.

According to the results of this study, it can be deduced that although using steel as a backing plate led to the increased in grain size and a large enhancement in the amount of the dislocation densities, but higher fracture load was achieved when steel was used as a backing plate. This can be imputed to the superior material mixing in the stir zone and the plastically deformed material flow zone. These results caused a significant betterment of the brazed zone (a defect-free weld was obtained).

The macroscopic images of the tensile/shear samples after fracture with steel and copper backing plates are represented in Fig. 15. It is noticeably obvious that the role of the backing plate on fracture mode is inordinately vital. Pin pull-out and circumferential fracture modes were

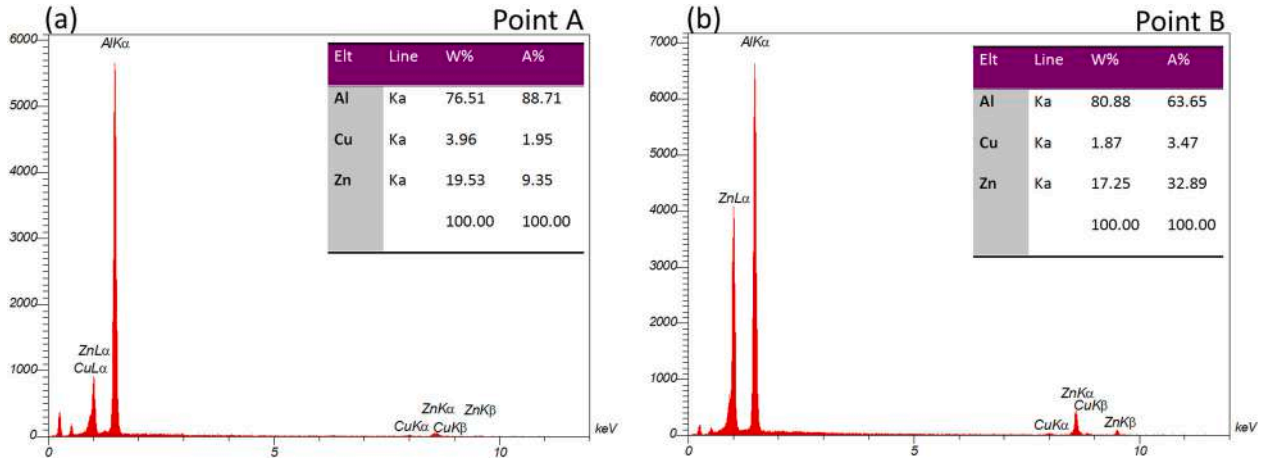

Fig. 18. EDS analyses of marked points on the fracture surfaces of the AA2024/Zn/Brass joint with steel backing plate.

observed. A gross disparity in the fracture mode from pin pull-out for the weld prepared by the copper to circumferential fracture mode for the weld prepared by steel backing can be another root cause in the mechanical behavior of the joints. It is important to note that the pin pull-out fracture mode confirmed the insufficient metallurgical bonding between Al and brass [11,12]. The schematic illustrations of the fracture path under tensile/shear loading are indicated in Fig. 15c and f. It is seen that the failure of the joint commences at the brazed zone and then propagates through Al and brass interface (the bond end), and the final fracture occurred (see red dotted arrows in Fig. 15c). Similarly, with the usage of the steel backing plate, failure commences at the brazed zone and then propagates towards the upper sheet and final fracture occurred in the shoulder indentation (see red dotted arrows in Fig. 15f). This fact corroborated that why the weld prepared using steel as a backing plate could offer a superfluous increment in the fracture load of the joints by 35% in comparison to the weld made by copper during the FSEB process of Al to brass.

The FESEM fracture morphology of the joints produced with steel and copper backing plates is revealed in Figs. 16 and 17. The fracture mode is primarily brittle regardless of the backing plate materials. However, the existence of tear ridges and numerous elongated dimples at the Al side confirmed the fracture mode was a mixed fracture, with a steel backing plate (see Fig. 16c and d). This fact depicts that the joint prepared by steel backing exhibited better load-bearing resistance and ductility more than the joint prepared by copper backing plate via the FSEB process. Besides, the EDS analysis from Fig. 16b proves that an Al-Zn eutectic structure is formed. The EDS results are provided in Fig. 18. Park et al. [10] reported that the lack of dimples in the fracture surface of the specimens is indicative of brittle fracture mode.

4. Conclusions

The friction spot extrusion brazing (FSEB) of AA2024-T3 aluminum alloy and brass was produced with a pure Zn as an intermediate material via the use of copper and steel backing plates. The impact of the backing plate materials on the microstructure, mechanical, and fracture behaviors of the welded AA2024/Zn/brass joint was explored in detail. The main conclusions of this study are summarized below:

- Backing plate materials played a vital role and altered the surface appearance (bottom side) in the friction stir extrusion brazed Al/Zn/brass joints. A complete filling of the pre-threaded hole via downward extrusion of the AA2024-T3 towards the brass side is achieved with steel backing, whereas the use of the copper as backing produced a relatively weaker interfacial bonding and poor plastic deformation. It was due to the low conductivity of steel than copper.
- Backing plate materials had a significant impact on the formation of the brazed zones at the edges of the joints, beneath the shoulder indentation in the friction stir extrusion brazed Al/Zn/brass joints. A sound weld without any interfacial defects was formed at the brazed zone with a steel backing plate that is attributable to increased heat loss when the copper backing plate was used as a backing plate.
- The change in the backing plate had a striking effect on the structure of friction stir extrusion Al/Zn/brass joint. Using a steel backing plate resulted in the formation of the Al-Zn eutectic structure at the brazed zone.
- Better fracture load is obtained by the steel backing plate even though the peak temperature enhanced with a alter in the backing plate material from copper to steel and subsequently resulted in the enhancement of the sizes of equiaxed recrystallized grains in the weld zone. The presence of Al-Zn eutectic structure in the brazing area and complete filling of the pre-threaded hole were the root causes for this phenomenon.

Declaration of competing interest

The results reported in the manuscript are original and neither the entire work, nor any of its parts have been previously published. The authors confirm that the article has not been submitted to peer review, nor has been accepted for publishing in another journal. The authors confirm that the research in their work is original and that all the data given in the article are real and authentic and there is no any conflict of interest. If necessary, the article can be recalled, and errors corrected.

References

[1] Boucherit A, Avettand-Fènoël M-N, Taillard R. Effect of a zn interlayer on dissimilar FSSW of Al and cu. Mater Des 2017;124:87–99.
[2] Abdollahzadeh A, Shokuhfar A, Cabrera JM, Zhilyaev AP, Omidvar H. The effect of changing chemical composition on dissimilar Mg/Al friction stir welded butt joints using zinc interlayer. J Manuf Process 2018;34:18–30.
[3] Ni Z, Zhao H, Mi P, Ye F. Microstructure and mechanical performances of ultrasonic spot welded Al/Cu joints with Al 2219 alloy particle interlayer. Mater Des 2016;92:779–86.
[4] Paidar M, Mohanavel V, Ojo OO, Mehrez S, Rajkumar S, Ravichandran M. Dieless friction stir extrusion-brazing (DFSE-B) of AA2024-T3 aluminum alloy to copper with zn interlayer. Results Phys 2021;24:104101.
[5] Paidar M, Memon S, Samusenkov VOlegovich, Babaei B, Ojo OO. Friction spot extrusion welding-brazing of copper to aluminum alloy. Materials Letters 2021; 285:129160.
[6] Kar A, Choudhury SK, Suwas S, Kailas SV. Effect of niobium interlayer in dissimilar friction stir welding of aluminum to titanium. Mater Charact 2018;145:402–12.
[7] Zhang Z, Li W, Shen J, Chao YJ, Li J, Mad Y. Effect of backplate diffusivity on microstructure and mechanical properties of friction stir welded joints. Mater Des 2013;50:551–7.

[8] Raja S, Manikumar R, Benruben R, Ragunathan S. Effect of backing plate on strength and microstructural characteristics of friction stir welded AA2014-T6 aluminum alloy joints. Mater Today Proc 2021;45:895–9.
[9] Paidar M, AshraffAli KS, Mohanavel V, Mehrez S, Ravichandran M, Ojo OO. Weldability and mechanical properties of AA5083-H112 aluminum alloy and pure copper dissimilar friction spot extrusion welding-brazing. Vacuum 2021;187:110080.
[10] Park SH, Joo YH, Kang M. Effect of backing plate materials in micro-friction stir butt welding of dissimilar AA6061-T6 and AA5052-H32 aluminum alloys. Metals 2020;10:933.
[11] Saju TP, Narayanan RGanesh. Dieless friction stir extrusion joining of aluminum alloy sheets with a pinless stir tool by controlling tool plunge depth. Journal of Materials Processing Technology 2020;276:116416.
[12] Saju TP, Ganesh Narayanan R. Dieless friction stir lap joining of AA 5050–H32 with AA 6061–T6 at varying pre-drilled hole diameters. J Manuf Process 2020;53:21–33.
[13] Skoko Ž, Popović S, Štefanić G. Microstructure of Al-zn and zn-Al alloys. Croat Chem Acta 2009;82:405–20.
[14] Paidar M, Mehrez S, Bokov D, Ramalingam VVignesh, Zain AMohd, Nasution MKM. The feasibility of friction stir spot extrusion-brazing of AA5083-H112 aluminum alloy to brass sheets with Zn interlayer. Materials Letters 2022;308(Part A):131084.
[15] Balasundaram R, Patel VK, Bhole SD, Chen DL. Effect of zinc interlayer on ultrasonic spot welded aluminum-to-copper joints. Mater Sci Eng A 2014;607:277–86.
[16] Huang G, Feng Z, Shen Y, Zheng Q, Zhao P. Friction stir brazing of 6061 aluminum alloy and H62 brass: evaluation of microstructure, mechanical and fracture behavior. Mater Des 2016;99:403–11.
[17] Paidar M, VairaVignesh R, Khorram A, OladimejiOjo O, Rasoulpouraghdam A, Pustokhina I. Dissimilar modified friction stir clinching of AA2024-AA6061 aluminum alloys: effects of materials positioning. J Mater Res Technol 2020;9:6037–47.
[18] Paidar M, Ghavamian S, Ojo OO, Khorram A, Shahbaz A. Modified friction stir clinching of dissimilar AA2024-T3 to AA7075-T6: effect of tool rotational speed and penetration depth. J Manuf Process 2019;47:157–71.
[19] Paidar M, Vignesh RVaira, Moharrami A, Ojo OO, Jafari A, Sadreddini S. Development and characterization of dissimilar joint between AA2024-T3 and AA6061-T6 by modified friction stir clinching process. Vacuum 2020;176:109298.
[20] Paidar M, Tahani K, Vignesh RVaira, Ojo OO, Ezatpour HR, Moharrami A. Modified friction stir clinching of 2024-T3 to 6061-T6 aluminum alloy: Effect of dwell time and precipitation-hardening heat treatment. Materials Science and Engineering: A 2020;791:139734.
[21] Liu F, Fu L, Chen H. High speed friction stir welding of ultra-thin AA6061-T6 sheets using different backing plates. J Manuf Process 2018;33:219–27.
[22] Chang CI, Lee CJ, Huang JC. Relationship between grain size and zener-holloman parameter during friction stir processing in AZ31 mg alloys. Scr Mater 2004;57:509–14.
[23] Rahmati Z, Aval HJ, Nourouzi S, Jamaati R. Effect of friction surfacing parameters on microstructure and mechanical properties of solid-solutionized AA2024 aluminum alloy cladded on AA1050. Mater Chem Phys 2021;269:124756.
[24] Paidar M, Oladimeji Ojo O, Moghanian A, Shaji Karapuzha A, Heidarzadeh A. Modified friction stir clinching with protuberance-keyhole levelling: a process for production of welds with high strength. JManuf Process 2019;41:177–87.
[25] Lei Hai Yang, Li Yong Bing, Carlson Blair E. Cold metal transfer spot welding of 1 mm thick AA6061-T6. Journal of Manufacturing Processes 2017;28:209–19.